

during the Paleocene-Eocene Thermal Maximum:

a case study using automated geometric morphometric methods to quantify tooth shape and size

Natasha Vitek¹, Carly Manz¹, Jonathan Bloch¹,
Douglas Boyer², Suzanne Strait³

¹Florida Museum of Natural History, Gainesville, FL, USA

²Duke University, Durham, NC, USA

³Marshall University, Huntington, WV, USA

Introduction

The Paleocene–Eocene Thermal Maximum (PETM) is marked by a rapid negative carbon isotope excursion with an associated shift towards warmer global temperatures by ~5–10 °C (Fig. 1; Secord et al 2012). At least 40% of the measured mammalian genera in the Bighorn Basin (BHB) are smaller during the PETM compared to adjacent, cooler biochrons, suggesting a relationship between climate change and body size (Secord et al., 2012). To date, only stasis in shape between biochrons was documented (Wood et al 2007). Within the PETM, size changes correlated with climate proxies have been documented in only one lineage (*Sifrhippus sandrae*) in the BHB (Fig. 1), and changes in shape were not addressed.

Here, we explore methods for quantifying both shape and size change at high stratigraphic and morphologic resolution.

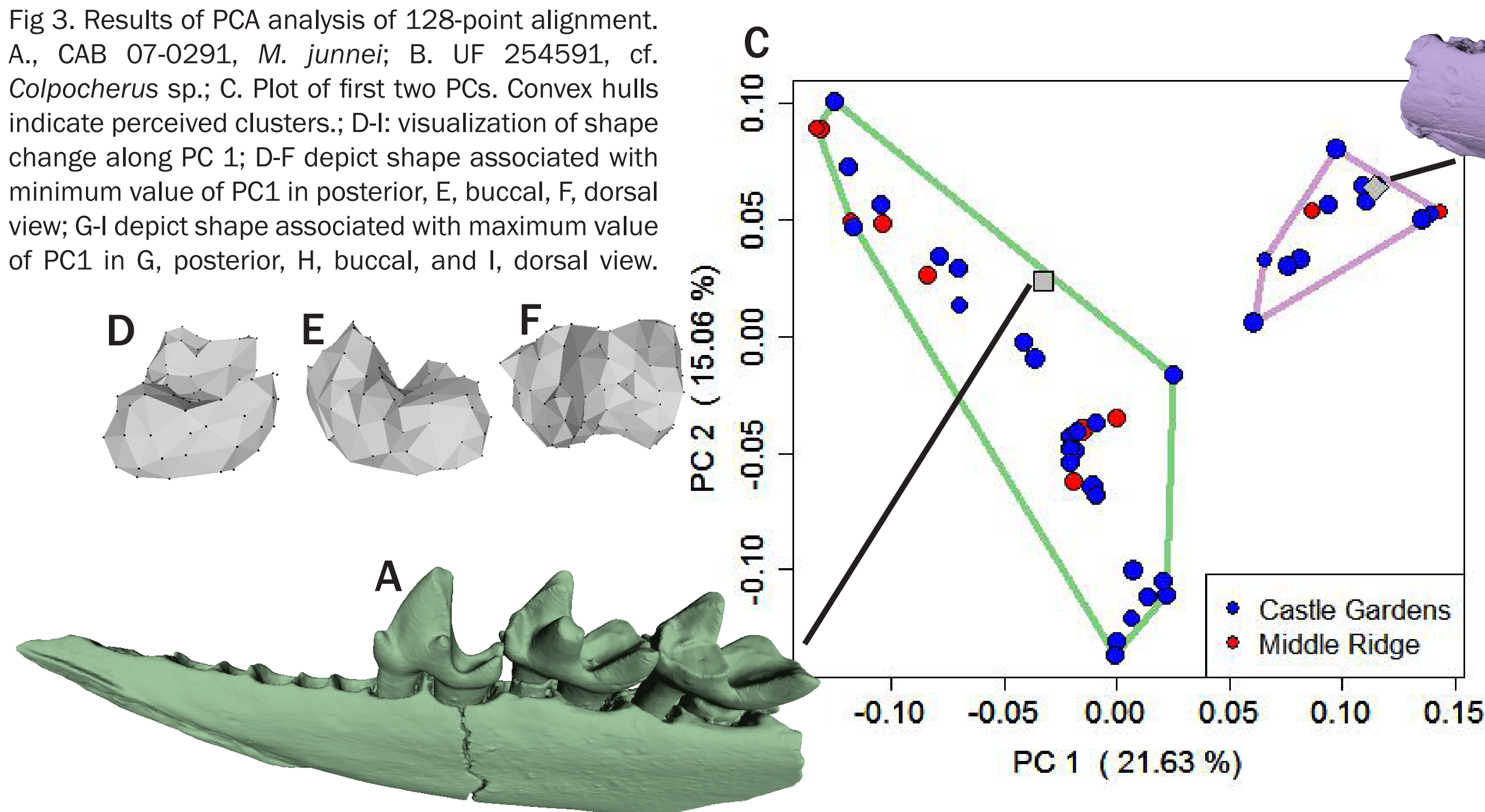
We use molars of *Macrocranion junnei* and cf. *Colpocherus* sp., two small-bodied taxa (~24 g; Smith et al. 2002; Rose et al. 2012), to explore method performance. The two taxa are most reliably identified by P/4 morphology (Rose et al., 2012). Their molars are difficult to differentiate.

Materials & Methods

- Two localities in the southern BHB were chosen, one from early in the Carbon Isotope Excursion (CIE; Castle Gardens locality, CG) and the other from late in the CIE (Middle Ridge locality, MR; Fig. 1).
- We used μ CT to digitize 48 M/1-M/2s with complete occlusal surfaces (Fig. 2A; CG n = 36, MR n = 10) including two specimens associated with P/4s (Fig. 3A-B).
- Digitized surfaces of each tooth were cropped to occlusal surface at the enamel-dentine junction using Avizo 8.1. Right molar surfaces were reflected to make all specimens “left” molars.
- In a departure from published methodology (Boyer et al, in press), all surfaces were downsampled to 10,000 faces to improve computation speed (Fig. 2B).
- R package auto3dgm (Boyer et al., in press) was used to automatically align surfaces and generate 128 3-D correspondence points (autolandmarks) per surface three times (Fig. 2C). Three alignments at 256 autolandmarks and one alignment at 512 autolandmarks were also generated. Aligned specimens were visually checked for alignment errors. Point clouds were analyzed in R with Welch’s T-tests, permutational MANOVA, and principal components analyses (PCA).

Results & Discussion

Fig 3. Results of PCA analysis of 128-point alignment. A., CAB 07-0291, *M. junnei*; B. UF 254591, cf. *Colpocherus* sp.; C. Plot of first two PCs. Convex hulls indicate perceived clusters.; D-I: visualization of shape change along PC 1; D-F depict shape associated with minimum value of PC1 in posterior, E, buccal, F, dorsal view; G-I depict shape associated with maximum value of PC1 in G, posterior, H, buccal, and I, dorsal view.



- The initial 128-point analysis produced shape variation along principal component (PC) 1 that corresponded to published differences between *M. junnei* and cf. *Colpocherus* sp. (Fig. 3D-I; Rose et al. 2012)

- Clusters were post hoc reidentified as either *M. junnei* or cf. *Colpocherus* sp. based on variation along PC1 and the positions of two M/1s with associated, diagnostic P/4s (Fig. 3A,B). Clusters occupy significantly different morphospace ($p < 0.001$).

- However, replicate 128-point alignments produced different, irreconcilable patterns of alignment (not shown), supporting the idea that initial clustering may be an artifact of low-precision alignment.

- Replicate 256-point alignments produced more tightly correlated PC1s than did 128-point alignments (Fig. 4).

- Tooth size did not differ between sites, regardless of alignment (Fig. 5).

- PCA of surfaces aligned at 512 points/specimen did not replicate previously identified clusters (Fig. 6).

Literature Cited

Beard, K.C., and M. R. Dawson. Early Wasatchian mammals of the Red Hot Local Fauna, uppermost Tuscaloosa Formation, Lauderdale County, Mississippi. *Annals of the Carnegie Museum* 78:193-243.
Boyer, D. M., J. Puentes, J. T. Gladman, C. Glynn, S. Mukherjee, G. S. Yapunich, and I. Daubechies. A new fully automated approach for aligning and comparing shapes. *Anatomical Record*.
Rose, K. D. 2006. The Beginning of the Age of Mammals. Johns Hopkins University Press, Baltimore. 431 pp.
Rose, K.D., A.E. Chew, R.H. Dunn, M.J. Kraus, H.C. Fricke, and S.P. Zack. 2012. Earliest Eocene mammalian fauna from the Paleocene-Eocene Thermal Maximum at Sand Creek Divide, southern Bighorn Basin, Wyoming. *University of Michigan Papers on Paleontology*, 36:1-122.
Secord, R., J. I. Bloch, S. G. B. Chester, D. M. Boyer, A. R. Wood, S. L. Wing, M. J. Kraus, F. A. McInerney, and J. Krigbaum. 2012. Evolution of the earliest horses driven by climate change in the Paleocene-Eocene Thermal Maximum. *Science* 335:959-962.
Smith, T., J.I. Bloch, S.G. Strait, and P.D. Gingerich. New species of *Macrocranion* (Mammalia, Lipotyphla) from the earliest Eocene of North America and its biogeographic implications. *Contributions from the Museum of Paleontology, University of Michigan* 30:373-384.
Wood, A.R., M.L. Zelditch, A.N. Rountree, T.P. Eiting, H.D. Sheets, and P.D. Gingerich. 2007. Multivariate stasis in the dental morphology of the Paleocene-Eocene condylarth Ectocion. *Paleobiology* 33:248-260.

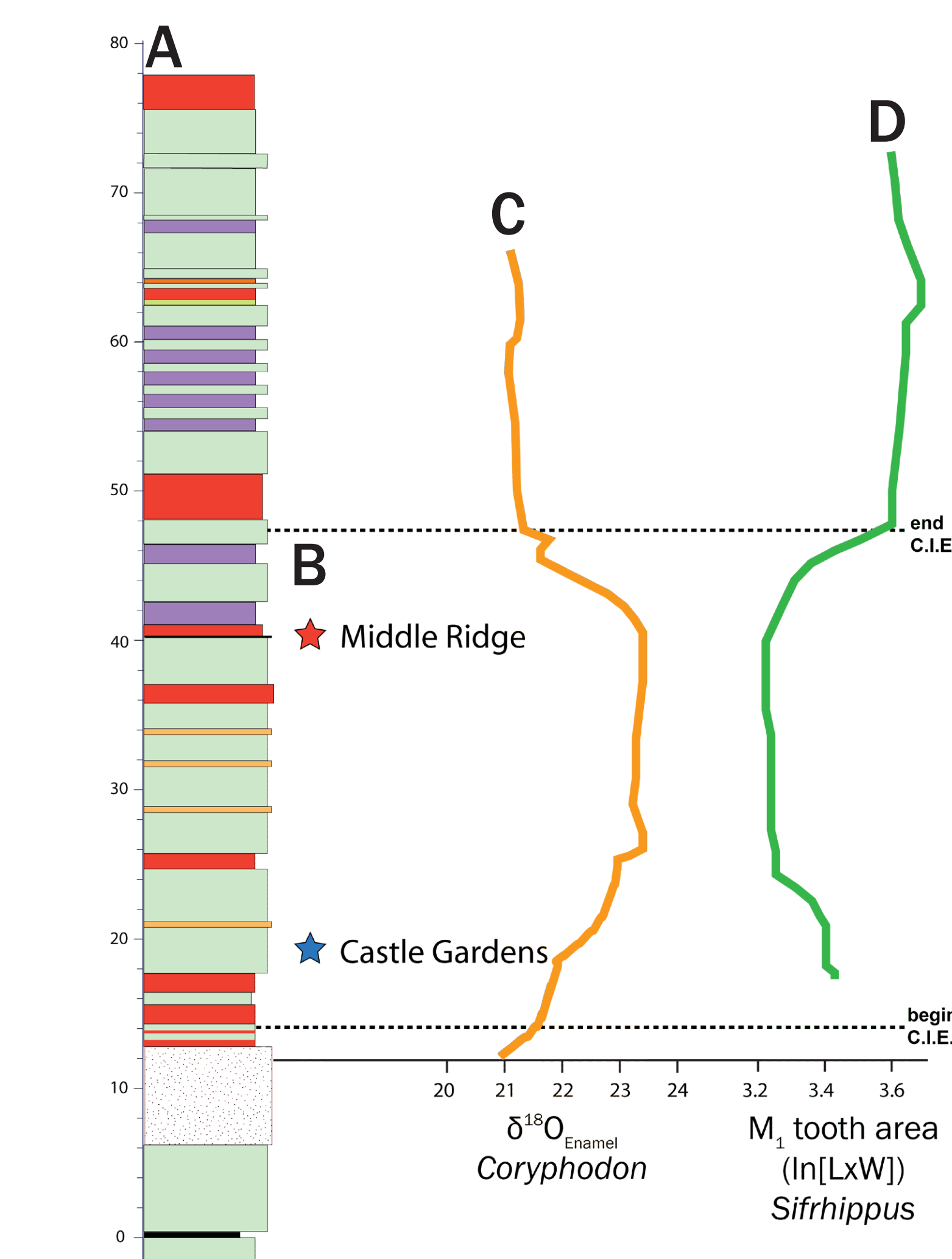


Fig. 1. The two localities used in this study in the context of stratigraphy, climate change, and the single previously documented high-resolution pattern of size change in vertebrates within the PETM. A., master stratigraphic section for the southern Bighorn Basin; B., stratigraphic level of sampled locality, labeled and colored to match results in Fig. 3; C., Five-point moving average of $\delta^{18}\text{O}$ values from tooth enamel of *Coryphodon*, as compared to the Vienna standard mean ocean water standard. Here, $\delta^{18}\text{O}$ values are a proxy for mean annual temperature. Larger values correspond to warmer conditions, or both; D, Five-point moving average of log-transformed measurements of first lower molar area of *Sifrhippus sandrae* (C and D redrawn from Secord et al., 2012). CIE = Carbon Isotope Excursion.

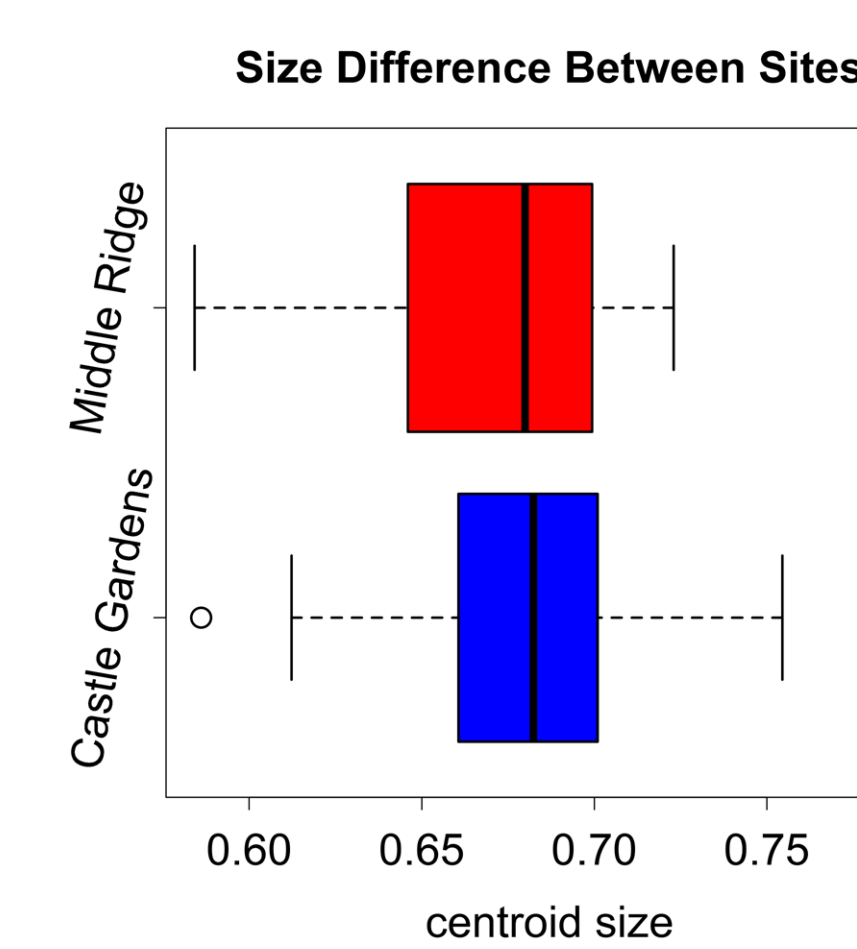
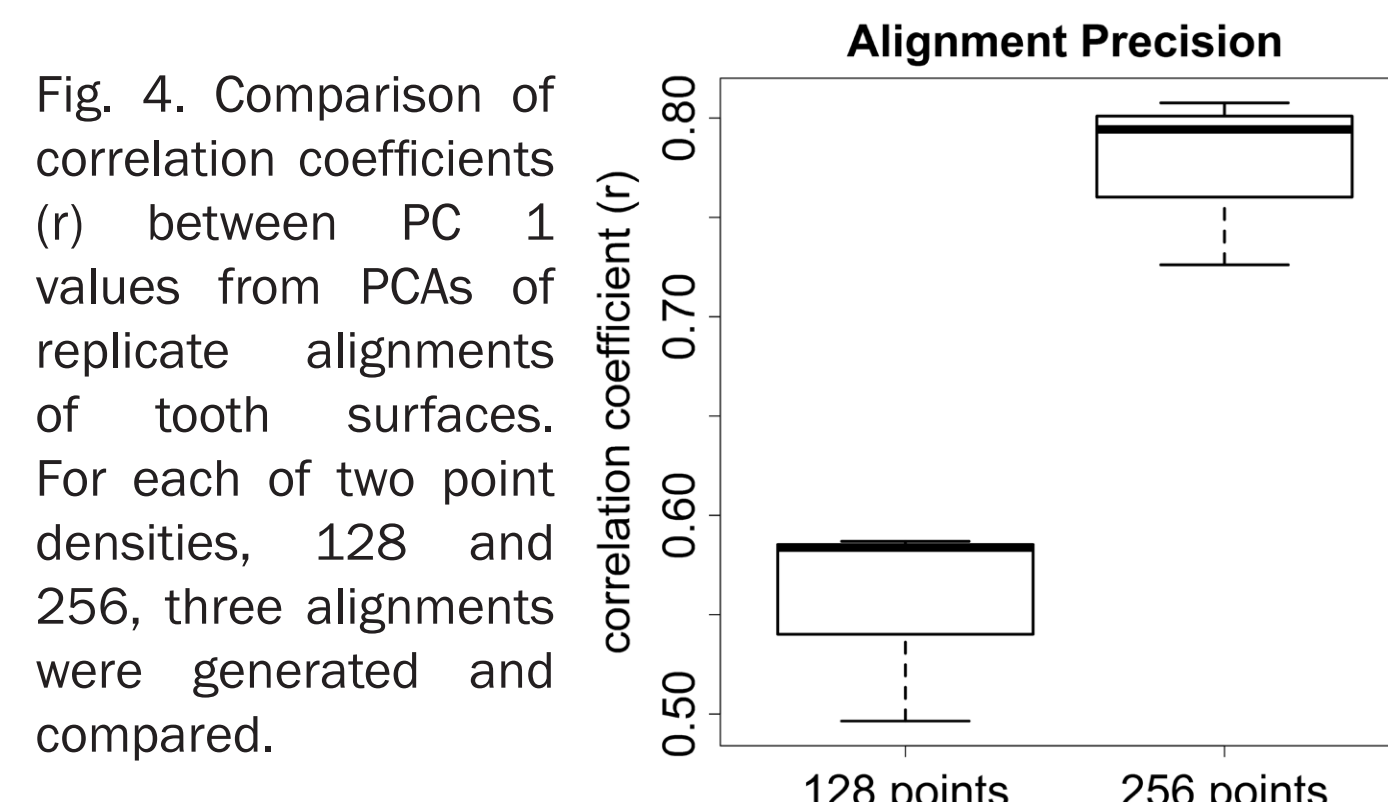
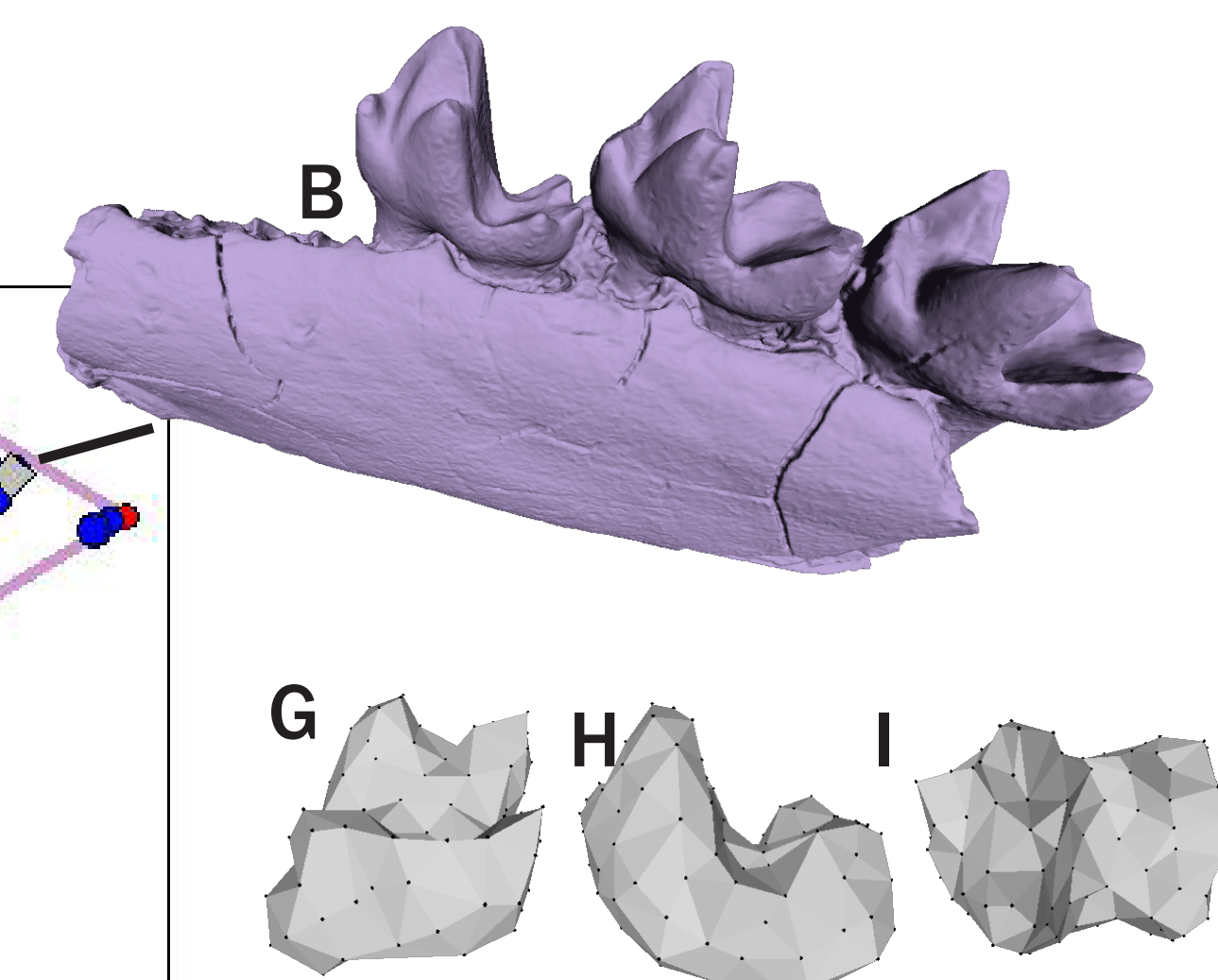


Fig. 5. Comparison of tooth size of pooled *M. junnei* and cf. *Colpocherus* sp. Scale is in unit centroid size, which is the square root of the summed distances to the center of the point cloud and which provides a size metric independent of shape.

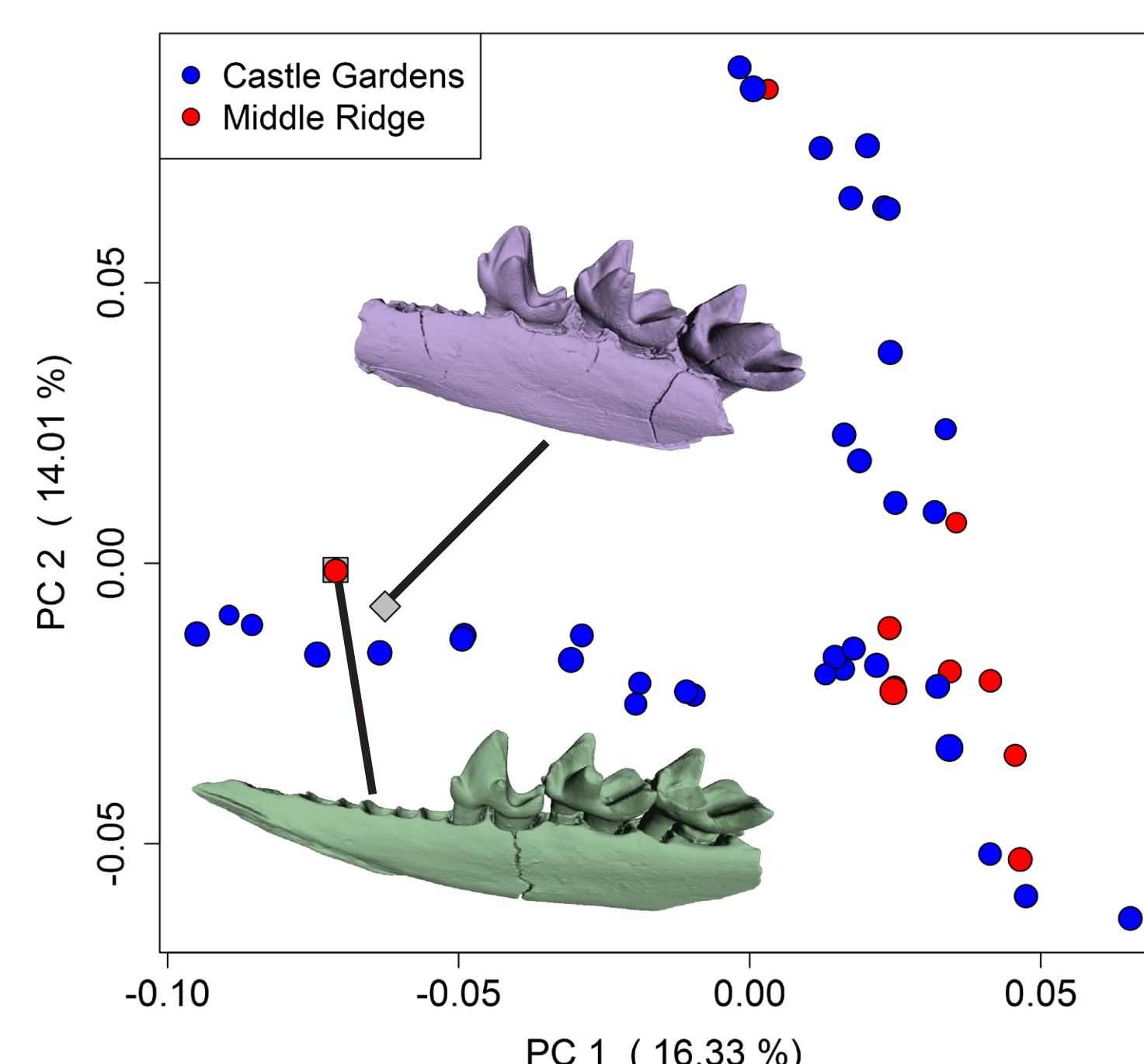


Fig. 6. Plot of first two PCs of PCA of 512-point alignment.

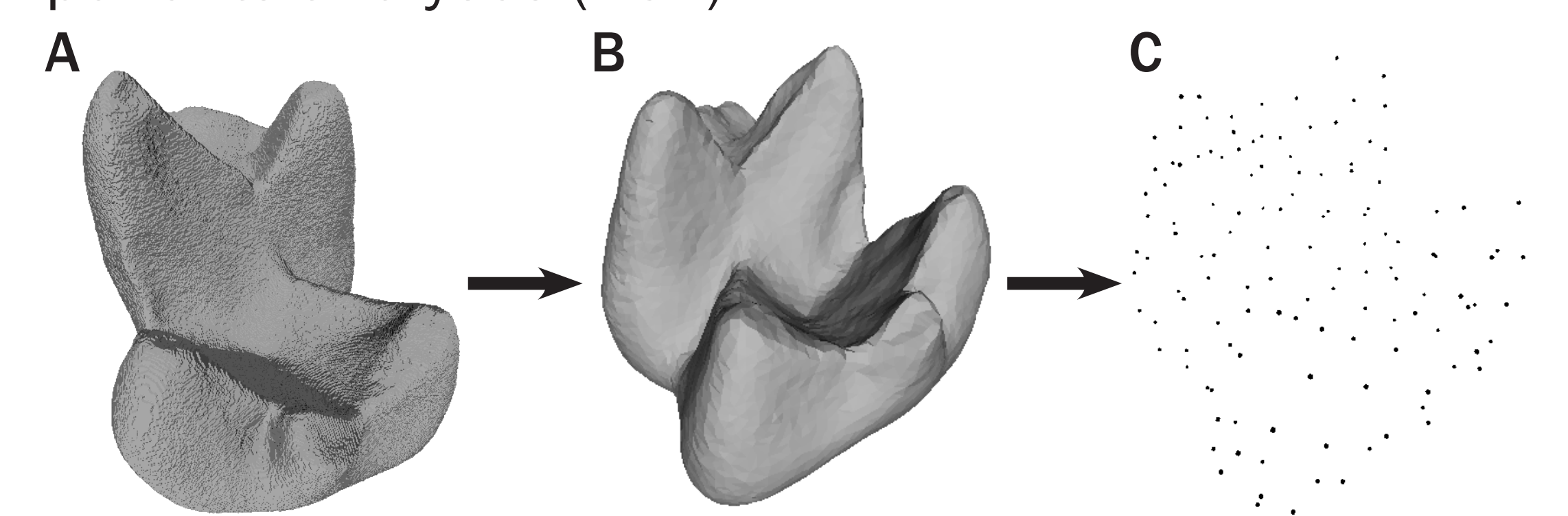


Fig. 2. Graphical summary of methods. A. μ CT-scan of the whole fossil UF 288308; B. Cropped occlusal surface of UF 283308, mirrored and downsampled to 10,000 faces; C. Cluster of 128 3-D correspondence points resulting from auto2dgm alignment of 57 specimens. Further analyses were performed using the point clouds as data.

Conclusions

- Though initial results appeared to confirm previous diagnoses of reference specimens as belonging to separate clusters, replicate analyses with 128 autolandmarks reveal this to be within the error of the procedure when aligning datasets of closely related shapes at this sampling density.

- Consistency of results, as reflected by correlation between principal components of replicate analyses, increases dramatically just by doubling the number of autolandmarks to 256. Boyer et al. (in press) used 1024 autolandmarks (8 times our initial count) and this clearly yields a consistent signal, but the analysis is slow. They did not validate intermediate levels of sampling.

- Patterns of static size in *M. junnei* and cf. *Colpocherus* sp. between sites with different climate regimes, regardless of alignment choice, are inconsistent with the pattern documented in *S. sandrae*.

Future directions:

- Continue to replicate more densely point-sampled alignments, find optimal balance between precision and computation speed. Continue developing methods to distinguish biological signal from noise.

- Analyze patterns of variation in P/4s of *M. junnei* and cf. *Colpocherus* sp. Both taxa might be examples of intraspecific variation in a single taxon (Rose et al. 2012).

- Increase taxon and locality sampling, because specimens of over 77 mammalian species in the high-resolution Cabin Fork BHB PETM section provide an opportunity to test whether taxa exhibit ‘individualistic’ or ‘coordinated’ responses to major climate perturbations.

Acknowledgments

Thanks to P. Holroyd for specimen access, A. Poyer for matrix picking, and members of the Cabin Fork field crew for digging, hauling, and washing matrix. This material is based on work supported by National Science Foundation Graduate Research Fellowship under Grant No. DGE-1315138 and a UF Lucy Dickinson Fellowship.